An Axial Gap Type self-bearing Motor with Separated Winding for An Implantable Maglev Pediatric Ventricular Assist Device

Yuki NAGASAWA*, Masahiro OSA*, Fumiya KITAYAMA*, Ryoichiro SATO* and Toru MASUZAWA*
*Graduate school of Science and Engineering, Ibaraki University
4-12-1 Nakanarusawa-tyo, Hitachi-shi, Ibaraki 316-0033, Japan
E-mail: masahiro.osa.630@vc.ibaraki.ac.jp

Abstract

Magnetically levitated motors have been applied as non-contact impeller suspension mechanisms in adult ventricular assist devices (VADs), indicating excellent blood compatibility. Recently, application of magnetic levitation in implantable pediatric VADs has been studied. However, miniaturization for small pediatric patients is difficult due to requirements of magnetic core shape, permanent magnet design, and winding arrangement in limited space. Therefore, magnetically levitated pediatric VADs are not clinically available yet. We have developed a self-bearing motor with an outer diameter of 22 mm and height of 43 mm using two 6-slot 4-pole permanent magnet synchronous motors for pediatric VADs. In previous research, an integrated winding was used for magnetic suspension and rotation, achieving non-contact impeller suspension. This configuration has high magnetomotive force but requires 12 windings excited independently by single-phase PWM current amplifiers, increasing size and power cable diameter.In this study, two insulated windings are arranged for each stator slot to construct a separated winding motor with two three-phase windings. Using four three-phase inverters, the total number of wires is reduced to 12. One winding is excited with four-pole control current, and the other with two-pole control current. The effect of this winding configuration on magnetic suspension stability was investigated. In this paper, the current control characteristics of the fabricated three-phase inverter are evaluated, and magnetic levitation tests are conducted using the separated winding motor and the three-phase inverter, The three-phase inverter has a bandwidth of 700 Hz. A maglev centrifugal blood pump with the separated winding motor was constructed and tested in a closed loop circulation circuit. Axial oscillation amplitude was suppressed within 0.06 mm, and inclination amplitude was less than 0.7 degrees.Non-contact suspension was achieved at all operating points. Future work will optimize the turns ratio of separated windings to enhance magnetic suspension performance and energy efficiency.

Keywords : pediatric ventricular assist device， maglev,self-bearing motor， separated windings, three-phase-inverter

1. Introduction

Magnetically levitated motors have been applied as non-contact impeller suspension mechanisms in adult ventricular assist devices (VADs) and indicating excellent blood compatibility in clinical use(J,Timothy Baldwin, et al, 2006 and Ono. M., 2009). In recent years, there has been a growing trend to use magnetic levitation technology in implantable pediatric VADs（C. Lin, X, et al, 2015, N. A. Greatrex, et al,2010 and Kevin Bourque, et al, 2001）. However, miniaturization of the magnetic levitation system to be implanted in small pediatric patients potentially has difficulty due to requirements of magnetic core shape, permanent magnet design and winding arrangement in limited space. Then, magnetically levitated pediatric VAD is not clinically available yet. We have developed a self-bearing motor with an outer diameter of 22 mm and a height of 43 mm using two 6-slot 4-pole permanent magnet synchronous motors for use in pediatric VAD. In previous research, we constructed a magnetically levitated motor that integrated windings for magnetic suspension and rotation, and non-contact impeller suspension was achieved(Yamaguchi, K., et al, 2021 and

Orihara, R., et al,2019 and Yamashita, T 2022). The integrated winding has advantages of maximizing the use of the winding for magnetic suspension and rotation control, resulting in a high magnetomotive force. In contrast, the 12 windings on the two stators are excited independently by a single-phase PWM current amplifier, which causes an increase in the size of the drive system and the diameter of the power cable of the VAD system. In this study, two insulated windings are arranged for each stator slot to construct a separated winding self-bearing motor with two three-phase windings, and the total number of wires is reduced to 12 by using four three-phase inverters. In this winding configuration, the deterioration of magnetic suspension performance and energy efficiency due to the reduction in magnetomotive force for magnetic suspension and rotation caused by the separated winding have to be considered. This paper investigated the magnetic suspension stability of the developed self-bearing motor using the separated winding to optimize magnetic suspension stability and energy efficiency.

2. Method

2. 1 Overview of the pediatric ventricular assist device using an ultra-compact self-bearing motor

The structure of the magnetically levitated pediatric VAD is shown in Fig. 1. The proposed pediatric VAD has top and bottom stators which have the same structure to provide non-contact magnetic suspension of the levitated impeller. The double stator structure achieves high torque production maintaining compact device size. An axial position (Z) and rotating speed (θz) of the levitated impeller are controlled by a four-pole rotating magnetic field, and radial positions (X, Y) and inclination angles around the radial axes of the levitated impeller are controlled by a two-pole magnetic field. By superimposing and distributing the control magnetic fields of four poles and two poles in the air gap, the five axes of the levitated impeller position and the rotation speed are actively controlled.

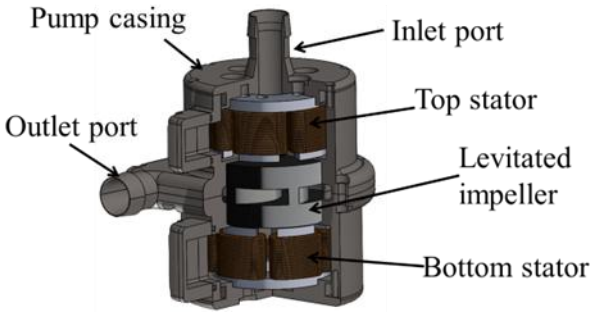

Fig.1 Structure of pediatric ventricular assist device

2.2 Principle of Magnetic Levitation Rotation Control of Self-bearing Motor

2.2.1 Principle of controlling axial position and rotation of levitated impeller

This motor produces axial suspension force and rotating torque based on vector control algorithm. The principle of generating axial suspension force is shown in Fig.2. The axial position (Z) is actively controlled by strengthening and weakening the magnetic field using d-axis current. It creates an imbalance in the magnetic suspension force between the top and bottom of the levitated impeller and generates an axial suspension force. The rotating torque (ω_z) is adjusted by the q-axis current.

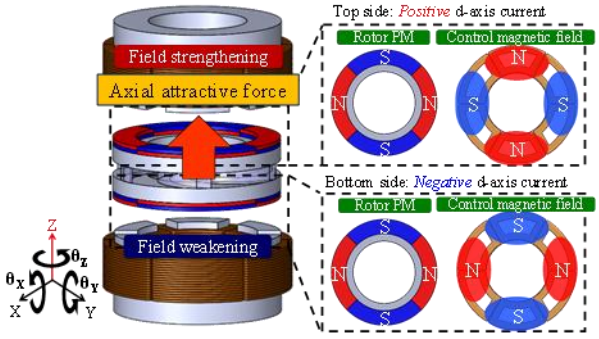

Fig.2 Principle of controlling axial position and rotation

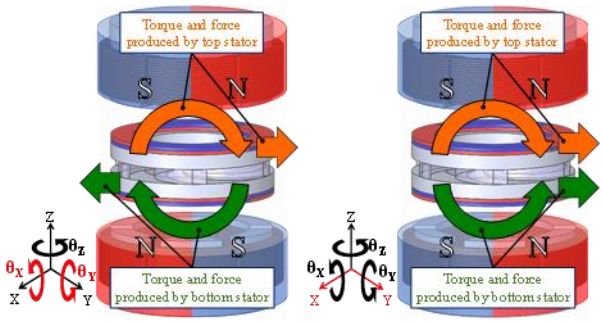

Fig.3 Principle of Inclination angle and radial position control

2.2.2 Principle of Inclination angle and radial position control of levitated impeller

Inclination angle (θ_x, θ_y) and radial position(X,Y) of the levitated impeller are controlled with P±2 pole theory. Fig. 3 shows the control principle of the inclination angle and radial position. The control magnetic field can simultaneously produce an inclination torque and a radial suspension force. Superimposing the inclination torque on the top and bottom stators cancels the radial support force, while superimposing the radial support force cancels the inclination torque. By adjusting these radial support forces and tilt torques, the radial position and tilt of the levitating impeller can be controlled independently. Axial gap motors are passively stable in the radial direction and can be driven by three-axis control.

2.2.3 Magnetic levitation and rotation control system

Fig.4 shows an overview of the magnetic levitation and rotation control system for this magnetically levitated motor. Three eddy current displacement sensors (PU-03A, Denshi Applied Electronics) are placed at 90° intervals on the inner side of the stator tooth to measure axial position and Inclination angle of the levitated impeller around the radial axis. Two eddy current displacement sensors placed on the sides of the levitated impeller measure the radial position. Three Hall sensors (HG-302C, Asahi Kasei Corporation) are set at 60° intervals in the slot of the bottom stator to detect the rotation angle of the levitated impeller every 30° in electrical angle.

Based on the levitated impeller position measured by each sensor, the control current is determined by a digital PID controller using dSPACE MicroLabBox and MATLAB Simlink, and each coil of the top and bottom motor stators is energized using a single-phase amplifier (Junus, JSP-090-10). This enables non-contact suspension and rotation of the levitated impeller.

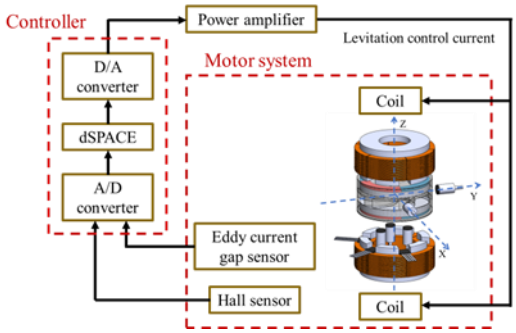

Fig.4 Magnetic levitation and rotation control system

2.3 Examination of motor winding configuration for simplification of the drive system of the self-bearing motor

As described in the previous section, in this self-bearing motor, to actively control the five axes of the levitated impeller position, the top and bottom stators generate a three-phase four-pole rotating magnetic field for axial position and rotation control and a three-phase two-pole rotating magnetic field for inclination angle and radial position control. When using the integrated winding, the control currents of the three-phase four-pole and three-phase two-pole windings are superimposed in the microprocessor and commanded to the single-phase amplifier to superimpose the rotating magnetic fields with different numbers of poles in the air gap. In the integrated winding drive, a total of 12 single-phase amplifiers are used in the top and bottom stators to apply control currents independently to each winding. To reduce the total number of wires and drive amplifiers, the separated winding motor was fabricated shown in Fig.5. In the separated winding motor, two insulated windings are arranged for one pole and the function is distributed to each winding. One winding is excited with a three-phase four-pole control current, and the other is excited with a three-phase two-pole control current. The two magnetic fields with different pole numbers are superimposed in the air gap. In this study, both windings have 58 turns in order to clarify the basic performance. Separated winding motors can be driven by a three-phase inverter by delta wiring.

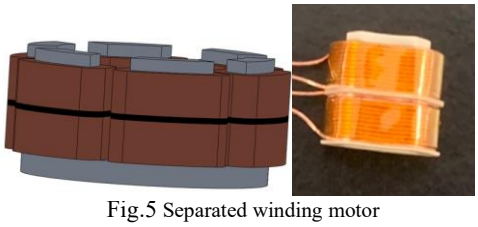

Fig.5 Separated winding motor

Fig.6 Three-phase inverter

2. 4 Overview of the Three-phase Inverter

Fig.6 shows the fabricated three-phase inverter (Desktop Labs, P13199-D1-001).The size of the inverter is 44× 55mm, and it is capable of exciting two systems of three-phase alternating current on a single board. The proposed drive system uses two boards to drive the motor. The proposed drive system can be smaller than conventional drive amplifiers, and the final goal is to develop a portable drive system that can be placed outside the body. Fig.7 and Fig.8 show block diagrams of the proposed drive system. The three-phase currents determined by the PID feedback loop are converted to two-phase currents by a Clarke transform. The converted two-phase currents are the command values to the three-phase inverter.

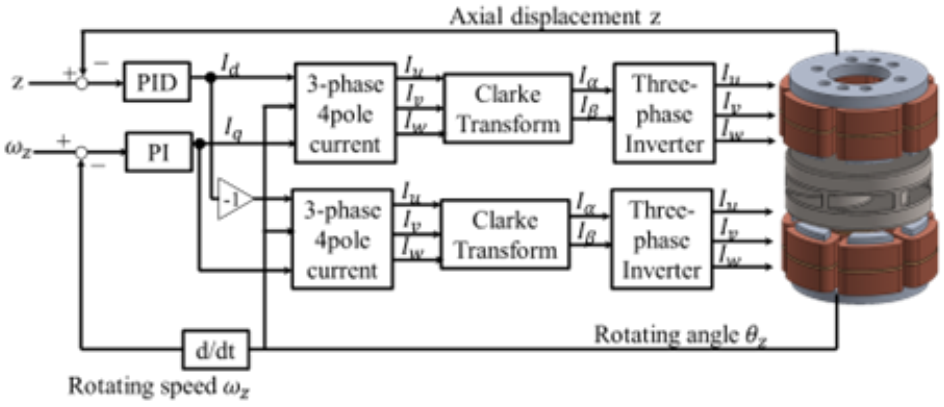

Fig.7 Diagram of the PID controller for the axial position and rotation

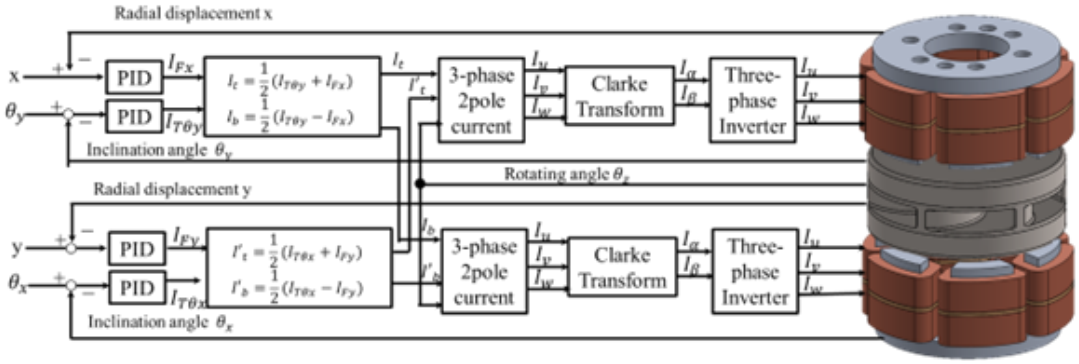

Fig.8 Diagram of the PID controller for the radial position and inclination

2.5 Overview of the proposed Pediatric Ventricular Assist Device

Fig.9 shows the prototype of the pediatric ventricular assist device consisting of a separated windings motor and centrifugal blood pump developed in this study. The outer diameter and height of the magnetic levitation motor are 22 mm and 35 mm, respectively. When the impeller is levitated at the axial magnetic center position, the air gap between the motor stator and the rotor is 1.3 mm. The length and width of the prototype pump is 42 mm and the height is 45.3 mm. The outer diameter of the levitated impeller is 23.2 mm, the height is 10.8 mm and the mass is 17.4 g. Double volute geometry is adopted to reduce the radial forces working on the impeller. The movable range of the rotor in the axial, radial, and Inclination angle is ±0.3 mm, ±0.7 mm and ±1.5 deg, respectively.

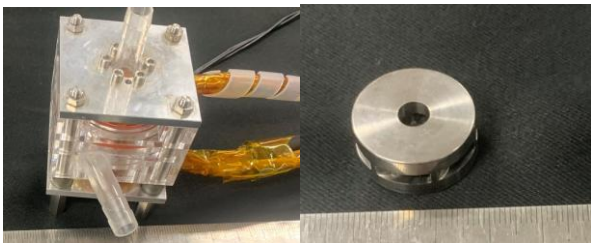

Fig. 9 Developed of magnetically suspended centrifugal pediatric ventricular assist device.

2.6 Evaluation of Current Control Characteristics of Three-Phase Inverters

Fig. 10 shows the experimental system for evaluating the current control characteristics of a three-phase inverter. Current control characteristics of the developed three-phase inverter evaluated with an FFT analyzer. Connect a separate winding motor to the three-phase inverter and input a sine wave as a current command value from the FFT analyzer. The current applied by the driving amplifier to the motor was measured by a clamp type current meter as the output to obtain a Bode diagram. The command value of the input signal was set to 1.0 A and the frequency varied from 10 Hz to 10 kHz.

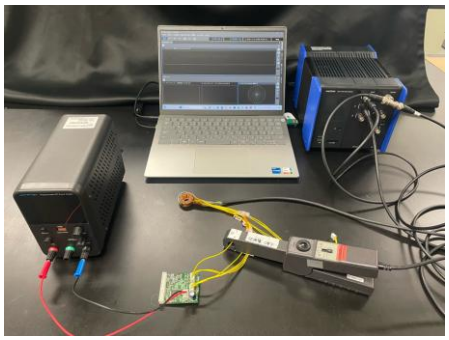

Fig.10 the experimental system for evaluating the current control characteristics

2.7 Evaluation of Pump Drive and Magnetic Levitation Characteristics

The fabricated pediatric ventricular assist device was connected to the closed loop circulation circuit shown in Fig. 11 to evaluate the levitated impeller position and motor power consumption. The circulation circuit consists of a reservoir bag, an ultrasonic flowmeter (Nipro Transonic, H12XL), a pinch valve, and a pressure gauge (NECAvio, 9E02-P13). The pump was driven by 3-axis control without radial position control in order to simplify the control system. Table 1 shows the control gains of the PID and PI controllers used for magnetic levitation and rotation. Since the number of control windings is half, the gain values used in this experiment were twice the values of the Integrated windings motor so that the magnetomotive forces are equal. The blood pump was driven at 3700 rpm, 4000 rpm, 4300 rpm, and 4600 rpm, and the pump flow rate was adjusted in 0.5 L/min steps by changing the resistance of the circulation circuit with a pinch valve, and the pressure difference between the pump inlet and outlet at each flow rate was measured as the head pressure. The control frequency of the magnetic levitation system and the sampling frequency of the measurement system were set to 10 kHz. The average of the maximum and minimum values of the axial position and tilt angle of the levitated impeller measured over a period of one second was calculated and used as the vibration amplitude. The total power consumption of the motor at each pump operating point was measured with a digital power meter (YOKOGAWA, WT1800).

Table 1 Digital PID control gains for posture control and rotation control

	P	I	D
Axial position	16 [A/mm]	0.1 [A/sec mm]	0.013 [A sec/mm]
Inclination angle	2.16 [A/deg]	0.0014 [A/sec deg]	0.003 [A sec/deg]
Rotation	0.001 [A/rpm]	0.0036 [A/sec rpm]	

Fig.11 Closed loop circulation circuit for magnetic suspension characteristics

3 Results

3.1 Evaluation of Current Control Characteristics of Three-Phase Inverters

The frequency response results are shown in Fig.12. The developed three phase inverter produced similar Bode diagrams irrespective of the excitation current wave height. The gain started to fall at approximately 400 Hz and the bandwidth was approximately 700 Hz. The peak gain was 0 dB and the gain margin at the phase crossover frequency was 7 dB.

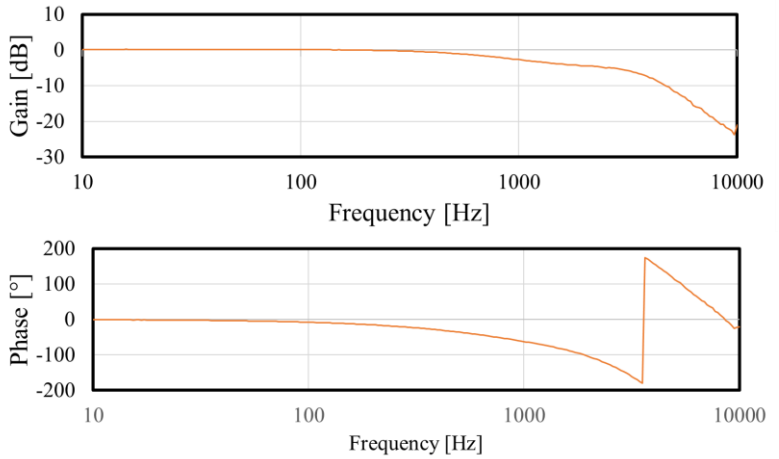

Fig.12 Frequency response

2.7 Evaluation of Pump Drive and Magnetic Levitation Characteristics

The pump characteristics of the prototype magnetic levitated pediatric ventricular assist device are shown in Fig.13. The pump could adjust the flow rate from 0.5 to 2.5 L/min for a head pressure of 80~100 mmHg at speeds in the range 3700-4600 rpm. Fig.14 shows the axial oscillation amplitude of the levitated impeller and Fig.15 and Fig.16 shows the inclination angle. The axial oscillation amplitude was suppressed between 0.03~0.06 mm overall operating points. The inclination amplitude was 0.5~0.7°. Although there was no impeller contact, the inclination amplitude was slightly larger than the allowable angle. The amplitudes of the axial position and inclination angle did not show any specific vibration. Fig.17 shows the command values of the q-axis current for the motor drive. The q-axis current generally increased linearly with increasing flow rate and rotation speed, ranging from 0.3~0.7 A. Fig.18 shows the RMS values of inclination control current. The values were 0.5~0.8 A. Fig. 19 show the total power consumption. Total power consumption increased with increasing flow rate and rotation speed. The power consumption in the range of the assumed operating point, was 1.7~4.5 W

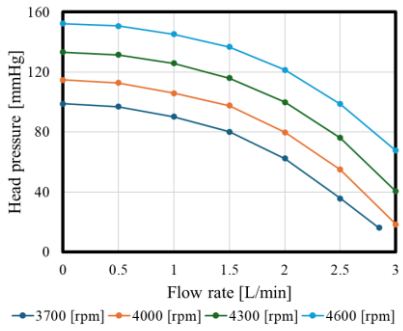

Fig.13 HQ characteristic

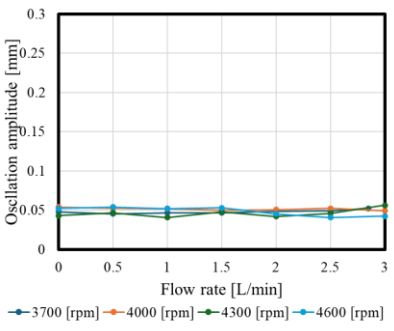

Fig.14 Axial oscillation amplitude

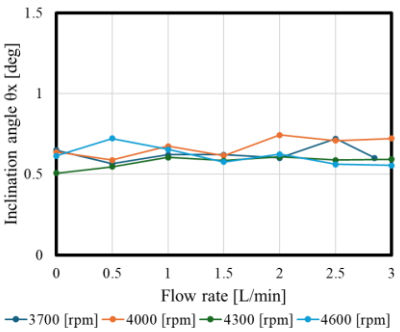

Fig.15 Inclination oscillation amplitude θ_x

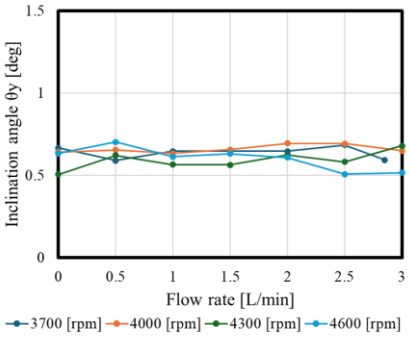

Fig.16 Inclination oscillation amplitude θ_y

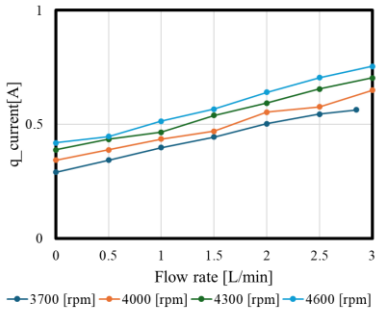

Fig.17 Motoring q-axis current

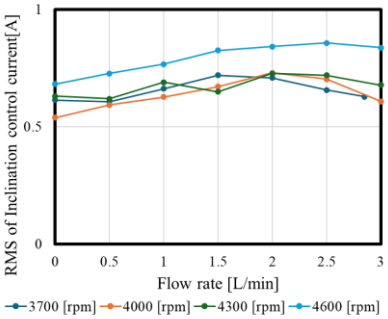

Fig.18 RMS value of inclination control current.

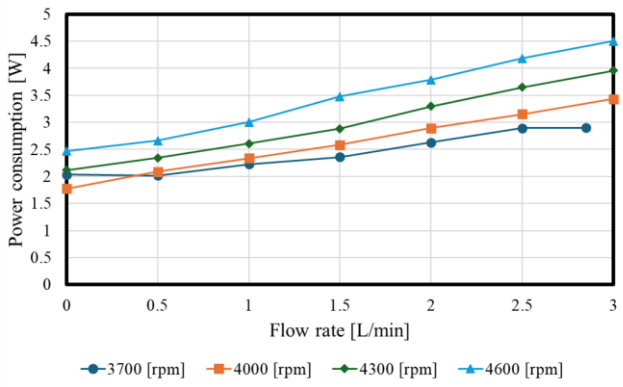

Fig.19 Power consumption

4. Discussion

4.1 Evaluation of Current Control Characteristics of Three-Phase Inverters

The assumed rotation speed of the maglev motor is approximately 3500-5000 rpm, and the frequency response is high enough to control the motor rotational frequency (117-167 Hz). On the other hand, the bandwidth is lower than the control and measurement frequency of 10 kHz in the magnetic levitation control system. It is therefore necessary to investigate the influence of the frequency response of this current amplifier on the dynamic characteristics of the impeller's non-contact support.

4.2 Evaluation of Pump Drive and Magnetic Levitation Characteristics

The separated windings motor achieves a non-contact pump drive at all measurement operating points. However, the inclination angle was found to be unstable with changes in flow rate and rotation speed. Consequently, Consequently, the current controlling the inclination angle increased with changes in flow rate and rotation speed. The cause of the instability of the tilt angle has not been clarified. The axial oscillation amplitude is stable so it cannot be attributed to an increase in amplitude due to a decrease in the number of turns. Reasons for tilt angle instability include (1) insufficient tuning of the three-phase inverter and (2) the possibility that noise generated during wiring connections interfered with the impeller position measurement sensor and caused disturbances in the levitation system. In the future, appropriate tuning of the drive three-phase inverter, frequency analysis of the measurement system noise and noise elimination will be carried out to achieve more stable levitation.

The number of control windings in the separated winding motor has been reduced from 116 to 58 turns. The control current required to generate the magnetomotive force increases two times. Since the load torque at the same pump operating point is the same regardless of the winding configuration, Copper losses increase by a factor of two because half the number of turns and the control current is doubled. The change in iron loss due to differences in the wiring method is small because the pump is driven in the same magnetic flux density conditions, Therefore, the difference in power consumption due to the different winding configurations is due to the increase in copper loss resulting from the reduction in the number of windings. In the present separated winding, the number of turns of the two windings is the same. In the future, we will analyze the required current for the magnetic support and motor drive of each axis in detail and study the turn ratio that minimizes power consumption to achieve energy conservation

5. Conclusion

The axial gap type double stator self-bearing motor with separated windings are developed for the implantable

maglev pediatric VAD. Non-contact impeller suspension of the blood pump with reduction of drive line cables by using four three-phase inverters are demonstrated. However, the deterioration of the inclination control was observed in the proposed configuration. Further stabilization of the magnetic suspension system with low energy input will be achieved by optimizing the ratio of the number turns of separated windings.

References

C. Lin, X. Liu, G. Wu, X. Hou, H. Li, C. Chen, P. Yang, Hematological, Biochemical, and End-organ effects of the CHVAD in Ovine Model, Proceedings of World Congress on Medical Physics and Biomedical Engineering, pp. 305-306, 2015.

J.Timothy Baldwin, Harvey S. Borovets, Brain W. Duncan, Mark J. Gartner, et al., The National Heart, Lung, and Blood In-stitute Pediatric Circulatory Support, Journal of the American heart association, pp. 147-155, 2006.

Kevin Bourque, David B. Gernes, Howard M. Loree II, J. Scott Richardson, et al., HeartMate III: Pump Design for a Centrifugal LVAD with a Magnetically Levitated Rotor, ASAIO Journal, Vol. 47, pp. 401-405, 2001

N. A. Greatrex, D. L. Timms, N. Kurita, E. W. Palmer, T. Masuzawa, Axial Magnetic Bearing Development for the BiVACOR Rotary BiVAD/TAH, IEEE Trans. Biomed. Eng., 57(3), pp. 714-721, 2010.

Ono. M., Current Status and Prospects of the Assistive Artificial Heart. Pediatrics (2009), Vol. 42, No. 5, pp. 36-37 (in Japanese).

Orihara,R, Masuzawa.T, Osa,M, Tatsumi,E, Improvement of the Compact Maglev Motor for Pediatric Ventricular Assist Device, journal of the Japan Society of Applied Electromagnetics and Mechanics (2019), Vol. 27, No. 2, pp. 219-224 (in Japanese).

Yamaguchi,K, Masuzawa.T, Osa,M, Tatsumi,E, Evaluation of Energy Saving on the Axial Maglev Motor for Pediatric Ventricular Assist Device, journal of the Japan Society of Applied Electromagnetics and Mechanics (2021), Vol. 29, No. 1, pp. 168-175 (in Japanese).

Yamashita,T, Masuzawa.T, Osa,M, Tatsumi,E, Nishinaka,T, Magnetic suspension performance and energy consumption characteristics of a maglev pediatric VAD using an ultra-compact axial gap type self-bearing motor with different number of actively controlled axes, journal of the Japan Society of Applied Electromagnetics and Mechanics (2022), Vol. 30, No. 2, pp. 117-123 (in Japanese).